NUMERICAL ANALYSIS OF FLOW AROUND RECTANGULAR CYLINDERS WITH VARIOUS SIDE RATIOS

Akira Rokugou[1*], Atsushi Okajima[2] and Isaac Gutierrez[3]

Three-dimensional numerical analysis of the flow around rectangular cylinders with various side ratios, D/H, from 0.2 to 2.0, was carried out for Reynolds number of 10^3 by using a multi-directional finite difference method on a regular-arranged multi-grid. The predicted results are in good agreement with the experimental data. It is found that fluid dynamic characteristics of rectangular cylinders alternate between the high-pressure mode and the low-pressure mode of the base pressure for D/H=0.2-0.6. We show that this phenomenon is induced by the change of the flow pattern around rectangular cylinders.

Keywords: Separated Flow, Wake, Vortex, Fluid Force, Rectangular Cylinder

1. INTRODUCTION

The flow around a circular or rectangular cylinder in the uniform flow is the most basic fluid dynamic phenomenon. It is known that the flow around a rectangular cylinder exhibits an unsteady behavior such as full-separation flow, alternately reattachment flow and full-reattachment flow, accompanied by a change in fluid dynamic force according to changes in Reynolds number and its side ratio, D/H, where D is the flow-direction length and H is the cross-flow direction length of a rectangular cylinder. In particular at high Reynolds number, Nakaguchi et al.[1] found by the wind tunnel experiment that drag coefficient and base pressure coefficient had peak values in a D/H=0.6 cylinder which has a flat cross flow section. Although, as in the work of Bearman et al.[2], many studies were carried out to resolve the above mentioned phenomenon at high Reynolds number of approximately $Re=10^4$. Recently, a fluid tunnel experiment in comparatively low Reynolds number region, $Re=(0.67\text{-}6.7)\times10^4$, was carried out by Ohya[3] and he found that the flow pattern around a rectangular cylinder with a side ratio D/H=0.5 was temporally and irregularly changed between the high-pressure mode and low-pressure mode of base pressure coefficient. Okajima et al.[4] carried out on experiment at low Reynolds number, $Re=10^3$, and found that the change in base pressure coefficient was dependent on Reynolds number by the wind tunnel studies. On the other hand, some numerical studies were recently carried out to resolve this phenomenon. Enya et al.[5] calculated the flow around rectangular cylinders with side ratios D/H=0.2-1.0 at high Reynolds number using the LES model. In this study, they simulated the same phenomenon in the experimental study of Ohya, and clarified the relationship between flow pattern and base pressure coefficient. Hayashi and Ohya[6,7] calculated the flow around rectangular cylinders with side ratios, D/H=0.4-0.6, at low Reynolds number, $Re=(1.0\text{-}3.0)\times10^3$, by the large-scale DNS with over 13 million mesh points. They used the high accuracy centered differencing scheme to non-equi-spacing grid for large calculation region especially in span-wise direction and found the same phenomenon in the case of high Reynolds number occurring at low Reynolds number.

In this study, numerical analysis of a three-dimensional flow field around rectangular cylinders with side ratios D/H=0.2-2.0, which involves D/H=0.6, the critical depth at high Reynolds

Received: July 9, 2004, Accepted: January 25, 2005.

1 YKK Corp., 200,Yoshida, Kurobe, Toyama, Japan.
2 Graduate School of Natural Sci. & Tech., Kanazawa Univ., 2-40-20, Kodatsuno, Kanazawa, Ishikawa, Japan.
3 Graduate Student, Graduate School of Natural Sci. & Tech., Kanazawa Univ., 2-40-20, Kodatsuno, Kanazawa, Ishikawa, Japan.
* Corresponding author. E-mail: a-rokugo@ykk.co.jp

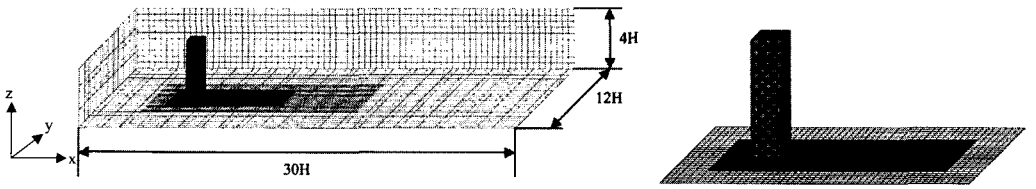

(a) Whole domain (b) Close-up view neighborhood rectangular cylinder

Fig. 1 Computational grid of D/H=1.0 cylinder

number, at comparatively low Reynolds number, $Re=10^3$, has been carried out. Then the changes of fluid dynamic characteristics with the side ratios at low Reynolds number have been compared with previous experimental ones. In particular, we have noted the relationship between flow pattern and base pressure coefficient nearby critical depth D/H=0.6, compared with the phenomenon at high Reynolds number.

2. NUMERICAL METHODS

2.1 GOVERNING EQUATIONS AND SCHEMES

A three dimensional continuity equation and Navier-Stokes equation, which is dimensionless by the representative velocity U_∞, where U_∞ is the free stream velocity, and the representative length H, where H is the depth of a rectangular cylinder, have been obtained as the governing equations. MAC algorithm has been used for the coupling between pressure and velocity. These governing equations have been approximated by a finite difference scheme. In these equations, the spatial differential terms, except for the convection term of Navier-Stokes equation, have been approximated by a second-order centered scheme. The convection term has been approximated by a third-order upwind scheme.[8] These spatial differential terms have been discretized on regular meshes using a multi-directional finite difference scheme[9] in order to achieve compatibleness of high accuracy and robustness. As using in past simulations, for example[8], a first-order Euler implicit scheme has been used for time integration. Calculated Reynolds number ($Re= U_\infty H/\nu$, ν describes kinematic viscosity of the fluid) is 10^3.

2.2 ANALYSIS CONDITION

An example of an analysis region is shown in Fig. 1 It spreads 6H for the upstream region, 24H for the downstream region, 6H for the side region from the center of a rectangular cylinder and 4H for the span wise region. This region is divided into four blocks and grid points are equally distributed in all spatial directions in each blocks; the minimum mesh size is 0.05H for the block adjacent to the cylinder and 0.4H for that in the outer region. Then the multi-grid method is used to combine these blocks in order to reduce calculation load by reducing the mesh number. Total mesh numbers are from about 2.5×10^5 (for D/H=0.2) to about 4.3×10^5 (for D/H=2.0). The boundary conditions are as follows; a uniform flow condition is obtained for the inlet, cyclic condition for the span-wise boundary and no-slip condition for the surface of the cylinder. We researched the various boundary conditions for the downstream and side boundary in previous study.[5] Then we decided the use of zero gradient condition for these regions.

3. ANALYSIS RESULTS

3.1 RESULT FOR D/H=0.2 CYLINDER

The time histories of drag, lift and base pressure coefficients affect to the D/H=0.2 cylinder is shown in Fig. 2 From temporary variations of drag and base pressure coefficients, it is shown that the mean value of base pressure coefficient increases, that of drag coefficient decreases and the amplitudes of fluctuations of these variables are weak from dimensionless times t=200 to 330. Corresponding to these phenomena, the amplitude of fluctuation of lift coefficient is small. On the other hand, for other times, each fluid force largely fluctuates, the mean value of drag coefficient is large and that of base pressure coefficient is small. The typical flow patterns of these two phenomena are shown in Fig. 3 and 4 Each flow pattern is shown by vorticity ω_z distribution, which has a span-wise axis, on the center plane of the x-y cross section. When the

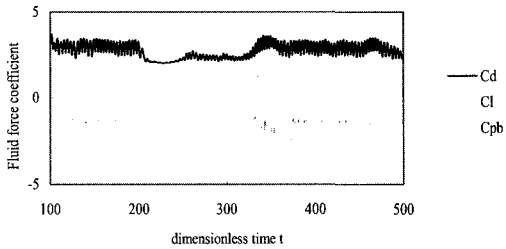

Fig. 2 Time history of fluid force of D/H=0.2 cylinder

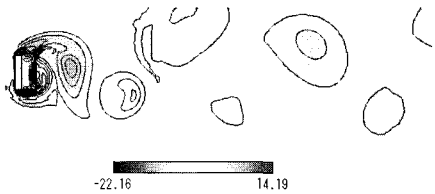

Fig. 3 Span-wise vorticity w_z distribution around D/H=0.2 cylinder (High-pressure mode, z=2.0H, t=300)

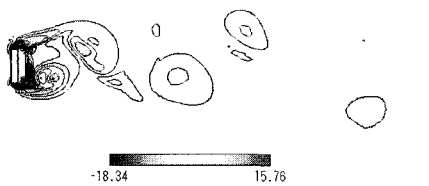

Fig. 4 Vorticity distribution around D/H=0.2 cylinder (Low-pressure mode, t=388)

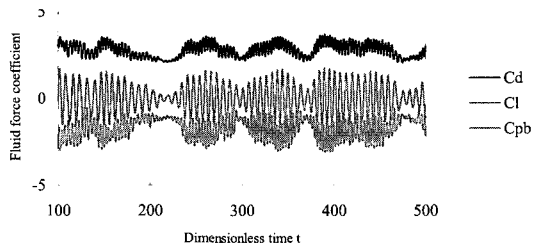

Fig. 5 Time history of fluid force of D/H=0.4 cylinder

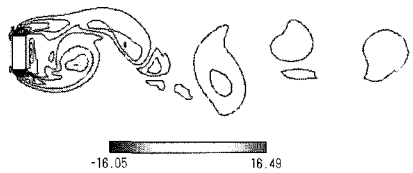

Fig. 6 Vorticity distribution around D/H=0.4 cylinder (High-pressure mode, t=226)

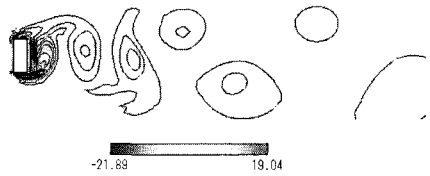

Fig. 7 Vorticity distribution around D/H=0.4 cylinder (Low-pressure mode, t=342)

mean drag coefficient is small and the mean base pressure coefficient is large, the flow separated from the leading edge forms vortex far away from the trailing edge of the cylinder. On the other hand, when the mean drag coefficient is large and the mean base pressure coefficient is small, the flow rolls up in a closer region from the trailing edge. However, in this case, a vortex is formed away from the trailing edge of the cylinder. Because the intensity of the latter vortex is stronger than that of the former, it is thought that the pressure fluctuation around the cylinder is larger and the amplitude of fluctuation is larger than former.

3.2 RESULT FOR D/H=0.4 CYLINDER

The time variations of fluid forces affect to the D/H=0.4 cylinder, as shown in Fig. 5 In this case, in contrast to the case of the D/H=0.2 cylinder, it is found that the pattern of large drag with low base pressure and that of small drag with high base pressure alternately appear in a short period. Moreover, the time of low base pressure is longer than that of high base pressure. The flow pattern of this case is shown in Figs. 6 and 7. In the case of high base pressure (shown in Fig. 6), similar to the case of the D/H=0.2 cylinder, the flow separated from the leading edge forms a vortex, which is large in the flow direction and diffusive, far away from the trailing edge of the cylinder. On the other hand, it is found that a vortex, which is small in the flow direction and has a strong intensity, is formed near the trailing edge of the cylinder by the flow separated from the leading edge in the case of low base pressure. Especially in latter case, being different from the case of the D/H=0.2, it is thought that the peak value of base pressure is lower as a result of the vortex formed much closer to the cylinder.

3.3 RESULT FOR D/H=0.6 CYLINDER

We show the results for the D/H=0.6 cylinder in Figs. 8 to 10. As shown in Fig. 8, the time history

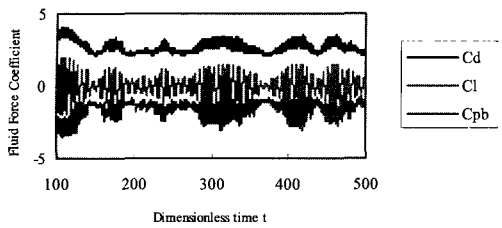

Fig. 8 Time history of fluid force of D/H=0.6 cylinder

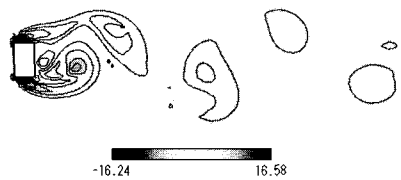

Fig. 9 Vorticity distribution around D/H=0.6 cylinder (High-pressure mode, t=377)

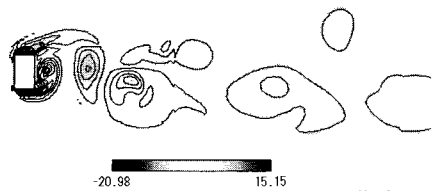

Fig. 10 Vorticity distribution around D/H=0.6 cylinder (Low-pressure mode, t=326)

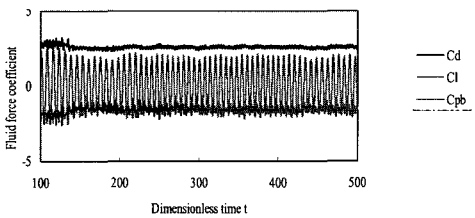

Fig. 11 Time history of fluid force of D/H=1.0 cylinder

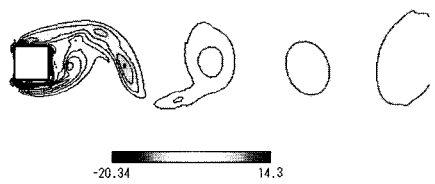

Fig. 12 Vorticity component w_z distribution around D/H=1.0 cylinder (t=371)

of fluid forces is similar to that of the D/H=0.4 cylinder and the pattern of large drag with low base pressure and that of small drag with high base pressure periodically alternate. In this case, it is

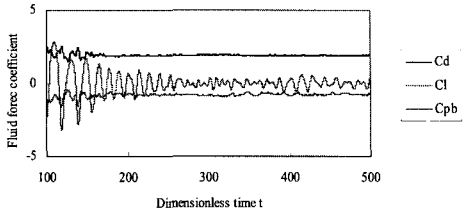

Fig. 13 Time history of fluid force of D/H=2.0 cylinder

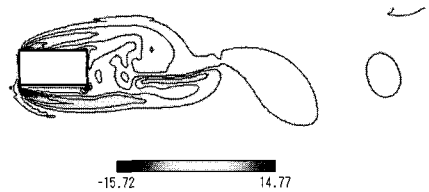

Fig. 14 Vorticity distribution around D/H=2.0 cylinder (Large fluctuation mode, t=234)

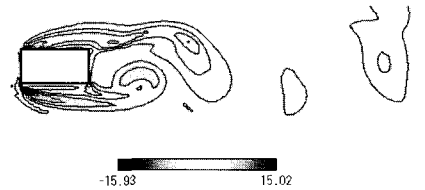

Fig. 15 Vorticity distribution around D/H=2.0 cylinder (Small fluctuation mode, t=329)

confirmed that the time rate holding the state of small drag with high base pressure is increased.

Therefore the mean drag coefficient takes a small value (2.637 for D/H=0.6 against 2.771 for D/H=0.4) and the mean base pressure takes a large value (-1.595 for D/H=0.6 against –1.733 for D/H=0.4). On the other hand, the variation of the flow pattern corresponding to this variation of fluid forces agrees with the case of the D/H=0.4 cylinder, as shown in Figs. 9 and 10.

3.4 RESULT FOR D/H=1.0 CYLINDER

The result for the D/H=1.0 cylinder, which has a square section, is shown in Figs. 11 and 12. It is found from the time history of fluid forces of the D/h=1.0 cylinder shown in Fig. 11 that drag, lift and base pressure coefficients exhibit an almost regular variation. This phenomenon is different from that in the case of D/H= 0.2 - 0.6 cylinders. As shown in Fig. 12, the flow pattern of the D/H=1.0 cylinder is as follows; the flow separated from leading edge rolls up far away from the trailing

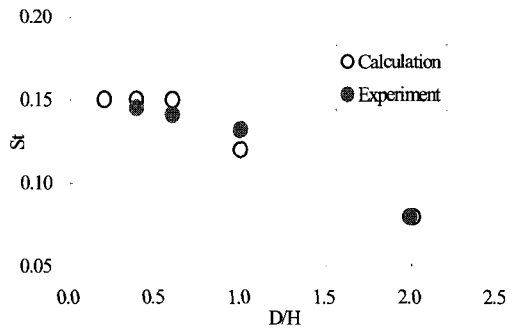

Fig. 16 Strouhal number variation with side ratio

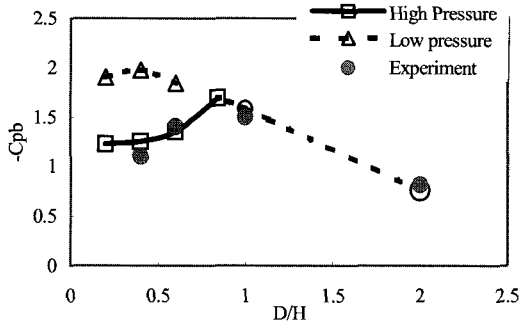

Fig. 17 Mean base pressure coefficient variation

edge of the cylinder and the Karman vortices regularly shed from there. It is thought from the time history of fluid forces and the flow pattern that the flow around a D/H=1.0 square cylinder corresponds to with large vortices forming of D/H=0.2-0.6 cylinders.

3.5 RESULT FOR D/H=2.0 CYLINDER

The result for the D/H=2.0 cylinder is shown in Figs. 13 to 15. As shown in Fig. 13, all fluctuations of fluid forces, drag, lift and base pressure, of the D/H=2.0 cylinder are very small and slow. In this case, the flow pattern changes as follows; the flow separated from the leading edge does not reattach to the side section of the cylinder, rolls up from the trailing edge and forms weak vortices.

Therefore, it is thought that the fluctuation of lift coefficient is controlled without forming a separation bubble beside the cylinder and the cycle of vortex shedding is long.

4. DISCUSSIONS

4.1 DEPENDENCE OF THE VARIATION OF FLUID FORCES ON SIDE RATIOS

First, the variation of vortex shedding Strouhal number ($St=fH/U_\infty$, f describes the wake vortex shedding frequency) and the mean of base pressure coefficient are shown in Figs. 16 and 17. The vortex shedding Strouhal number is almost constant value for the D/H=0.2-0.6 cylinders, then decreases as side ratios increase. As observed in Fig. 16, the result of this simulation shows good agreement qualitatively and quantitatively with experimental ones obtained by Okajima et al.[4] On the other hand, since there are two patterns, which have high and low base pressure modes as mentioned above, two values for each pattern are plotted in Fig. 17. Concerning this, though the value of the D/H=0.4 cylinder is slightly large, it is confirmed that this calculation result qualitatively and quantitatively is in good agreement with experimental data.[4] Therefore, it is thought that this calculation result simulates fluid dynamic characteristics against the change in side ratio.

4.2 TWO CHARACTERISTIC MODES; LOW-PRESSURE AND HIGH-PRESSURE MODES

It is confirmed by high Reynolds number analysis[5] that the mode of the large drag coefficient with low base pressure coefficient and that of the small drag coefficient with high base pressure coefficient appears alternately. Thus, we would like to verify the phenomenon at low Reynolds number from this calculation result. Fig. 18 shows the vorticity contour of ω_x for the high-pressure mode of the D/H=0.4 cylinder, and Fig. 19, that for the low-pressure mode of the same cylinder respectively. Moreover, vorticity contour is in the y-z section 3H from the trailing edge of the cylinder. In the high-pressure mode shown in Fig. 18, vortices which have positive and negative values alternately form a line in an almost equal distance of z=2.0H, shown corresponding to the vorticity contour of ω_z in Fig. 6. The vortex forming of ω_z rolls up in the downstream region, and vorticity distribution widely spreads in the span-wise direction and is diffusive similar to that of ω_z. On the other hand, in the low-pressure mode shown in Fig. 19, similar to the high-pressure mode, vortices which have positive and negative values stand in a line in equal distance of z=1.3H. It shows similar trend to ω_z that is observed the distribution is wide

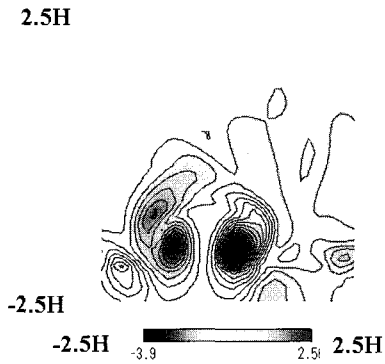

Fig. 18 Stream-wise voticity component w_x distribution behind D/H=0.4 cylinder (High pressure mode, x=3.2H, t=226)

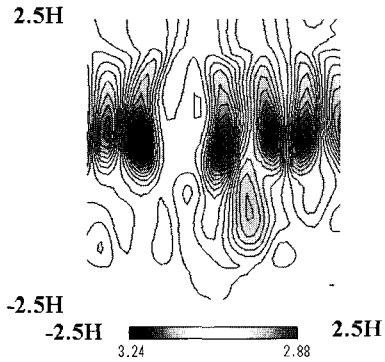

Fig. 19 Vorticity distribution behind D/H=0.4 cylinder (Low pressure mode, t=342)

in the height direction and narrow in the span wise direction. Although the peak value of vorticity is nearly equal in the high-pressure and low-pressure modes, vortices, which have large distribution and are diffusive, are formed in the high-pressure mode and those, which have narrow distribution and are condensed, are formed in the low-pressure mode. As a result, the fluctuations of the fluid forces of the rectangular cylinders and their fluctuation are large. This variation of the flow pattern is similar to that in high Reynolds number[5] and it is found that fluid dynamic characteristics are affected by the three-dimensional vortex structure of flow in low Reynolds number of Re=10^3. Moreover, in the case of the D/H=1.0 cylinder, it is confirmed in Fig. 20 that vortices are formed similar to that in the low-pressure mode and as a result, it is thought that fluctuation of lift coefficient is large. In the case of the D/H=2.0 cylinder, it is shown in Fig. 21 that

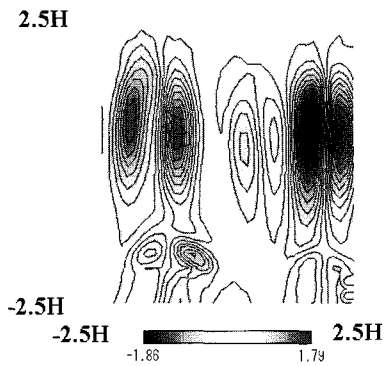

Fig. 20 Vorticity distribution behind D/H=1.0 cylinder (x=4.0H, t=371)

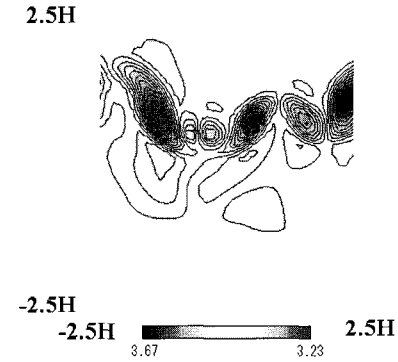

Fig. 21 Vorticity distribution behind D/H=2.0 cylinder (x=5.0H, t=234)

vortices have wide distribution in the span wise direction, thus it is thought that fluctuation of fluid force is extremely small.

5. CONCLUSIONS

The flow around rectangular cylinders with various side ratios, D/H=0.2-2.0, in Reynolds number Re=10^3 was numerically analyzed using multi-directional finite difference and multi-grid methods. The following are the result obtained.

The calculation results are compared with experimental results; the propriety of the calculation method used is confirmed since the calculation results agree qualitatively and quantitatively with the experimental results.

It is found for the D/H=0.2-0.6 cylinders that the phenomenon which takes peak values of base pressure and drag is caused by the temporally alternating mode which has low base pressure with

large drag and high basle pressure with small drag, and it is confirmed that this phenomenon is similar to that in high Reynolds number.

It is found that the effect of magnitude of fluid forces of rectangular cylinders is changed by vortex shedding which forms condensed and strong vortices in the low-pressure mode and diffusive and weak vortices in the high-pressure mode.

REFERENCES

[1] Nakaguchi, H., Hashimoto, K. and Muto, S., 1968, *J. Jpn. Aero. Soc*, Vol.16, No.168, pp.1-5.

[2] Bearman, P.W. and Trueman, D.M., 1972, *Aeronautical Quarterly*, Vol.23, p.229.

[3] Ohya, Y., 1994, *J. Fluids & Structures*, Vol.8, p.325.

[4] Okajima, A., Kimura, S., Ohtsuyama, S. and Ojima, A., 1998, *J. Struct. Eng. JSCE*, Vol.44A, pp.971-977.

[5] Enya, A., Okajima, A. and Rokugou, A., 2002, *Trans. Jpn. Soc. Mech. Eng.*, Vol.68, No.670, pp.1601-1607.

[6] Hayashi, K. and Ohya, Y., 2001, *Proc. 2001 Meet. Jpn. Soc. Fluid Mech.*, pp.608-609.

[7] Hayashi, K. and Ohya, Y., 2002, *Proc. 2002 Meet. Jpn. Soc. Fluid Mech.*, pp.348-349.

[8] Kawamura, T. and Kuwahara, K., 1984, *AIAA paper*, pp.84-340.

[9] Kuwahara, K., 1999, *AIAA paper*, pp.99-3405.